PNAS
www.pnas.org

Supplementary Information for

Scale-free movement patterns in termites emerge from social interactions and preferential attachments

Leticia R. Paiva, Alessandra Marins, Paulo F. Cristaldo, Danilo Ribeiro, Sidiney G. Alves, Andy Reynolds,Og DeSouza, Octavio Miramontes

Corresponding Author Og DeSouza
E-mail: og.souza@ufv.br

This PDF file includes:

Supplementary text
Figs. S1 to S14
Legends for Movies S1 to S2

Other supplementary materials for this manuscript include the following:

Movies S1 to S2

Supporting Information Text

Raw data will be made available at Harvard Dataverse (https://dataverse.harvard.edu/).

Social interactions and collective behaviours

As the density of the arena is increased, termite workers tend to cluster tightly. Under these conditions individuals effectively decrease their moving speed in order to engage in social interactions so that the probability of truncating their otherwise free trajectories is increased as well. This situation is, however, highly dynamic as cluster of different sizes persistently form and disintegrate afterwards. Individuals in the border of a cluster may detach from it but individuals in the center, albeit not often, would also spontaneously walk slowly and find their way out from the cluster to explore the arena. Individuals freely walking far from the cluster may come across the cluster in its way and may attach to it or not, preferentially (see the following VIDEO| 5:03 min, as an example).

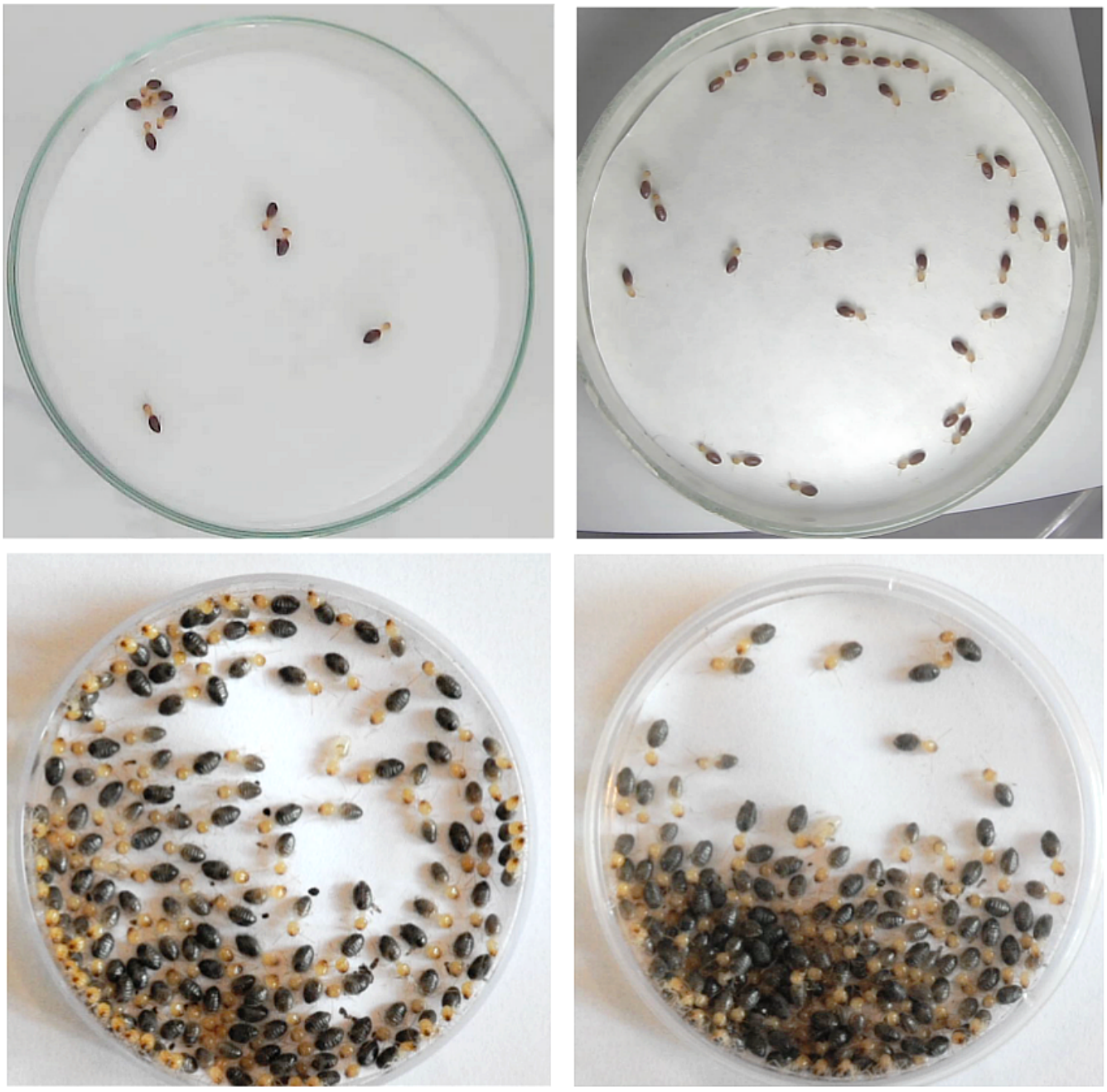

Fig. S1. Examples of termite groups of different sizes forming as the density is increased. Notice also separate individuals wandering around while exploring a Petri dish of diameter 53 mm.

Social trapping –or social jamming– may well be a term to describe this process of attaching and detaching from a cluster, since it is modulated by social interactions. Social trapping induces waiting times while the individuals stands still (these waiting times are known to be power law distributed [1]). It is also a factor to induce the shortening of the exploration steps and so it is the collective mechanism that induce a statistical distribution of steps lengths described by power laws, as described in the text. A graphical evidence of the emergence of Lévy trajectories patterns can be seen in the examples depicted in Figure S2. An extra observational experiment was performed where around 400 workers were located on a large rectangular arena (60x40cm). In this experiment, all individuals were initially located at the center of the container and were allowed to move from there. Initially they tend to move away until reaching the edges, after an initial transient time, the arena was characterized by a heterogeneity in the density and size of social clusters and a number of moving individuals hopping among them when detaching and re-attaching. No large clusters were observed but multiple small clusters, this suggests strongly that individuals attach preferentially and do not interact all-against-all, simultaneously (see the following VIDEO| 20:00 min, as an example)

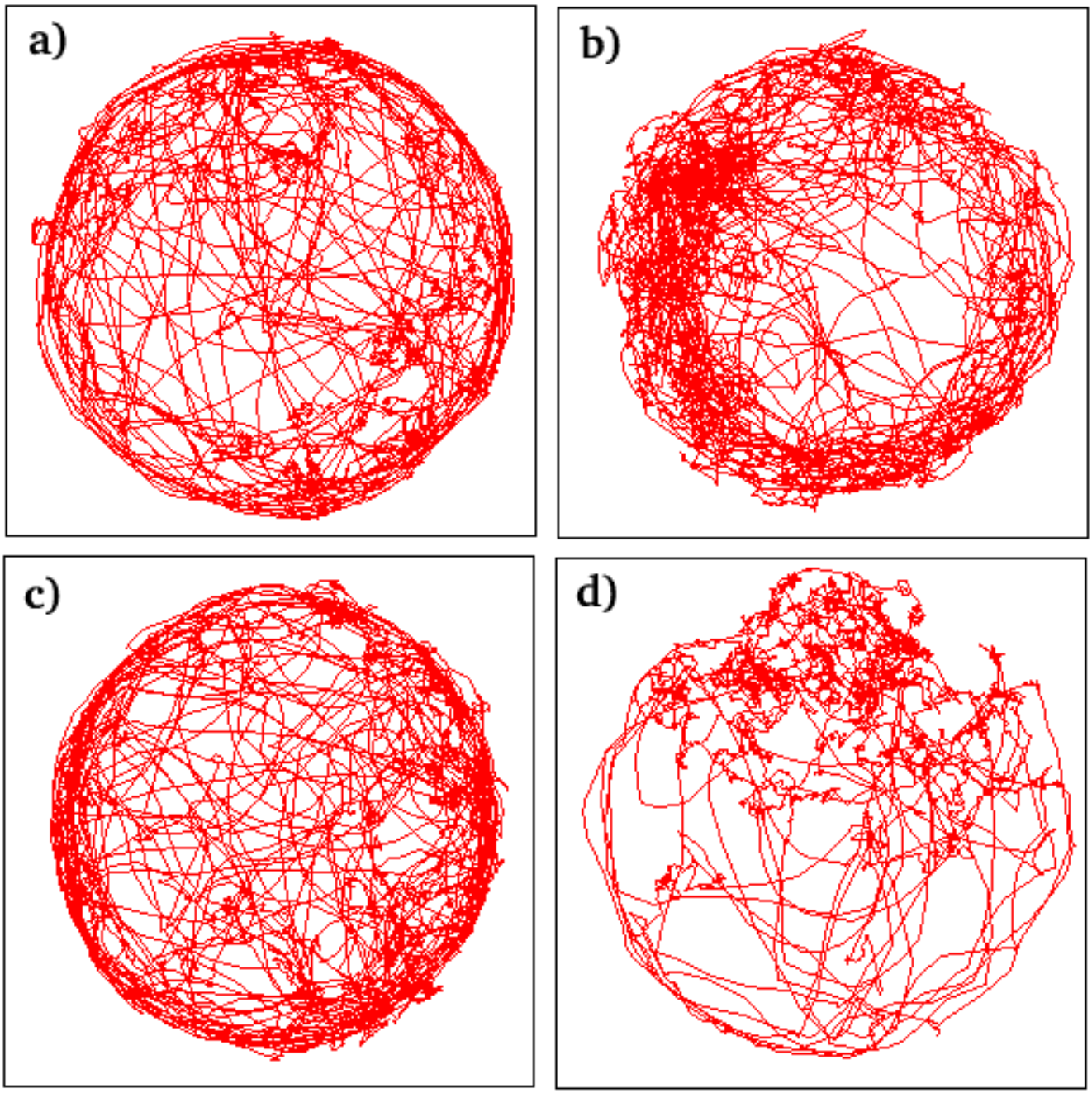

Fig. S2. Visual emergence of Lévy trajectories as the density of workers in the container arena is increased. Individuals wander around while exploring the Petri dish of diameter 53 mm. Notice that in the low density situation (a), the worker trajectory is mostly ballistic where large steps dominate. In (d) the focal individual have its trajectories truncated when engaging in social interactions with another individuals. Group sizes are (a) 12, (b) 15, (c) 18 and (d) 29 individuals in a 53 mm Petri dish.

Motion with inert passive obstacles

In order to test if the emergence of Levy walks could be due to non social mechanical stimulation rather than social interactions, a null experiment was designed where inert obstacles were introduced in the arena, as shown in Fig S3, in a range of densities and different spatial configurations. Only one termite was introduced and tracked, no social interactions are present but only space restrictions due to the obstacles.

Sandblasted glass arenas with an upside down 53mm diameter Petri dish as cover were used and 1, 10, 13, 16 and 29 obstacles were introduced glued into the arenas. Each of these obstacles is a cylinder made of steel with 9.3 mm height and cross-section area equals to 19.59mm^2, close to the mean area occupied by a termite, estimated as 18.53mm^2 (antennae and "legs" considered). The steel was chosen as it has a smooth surface, so the termite was not able to climb it, and it is chemically

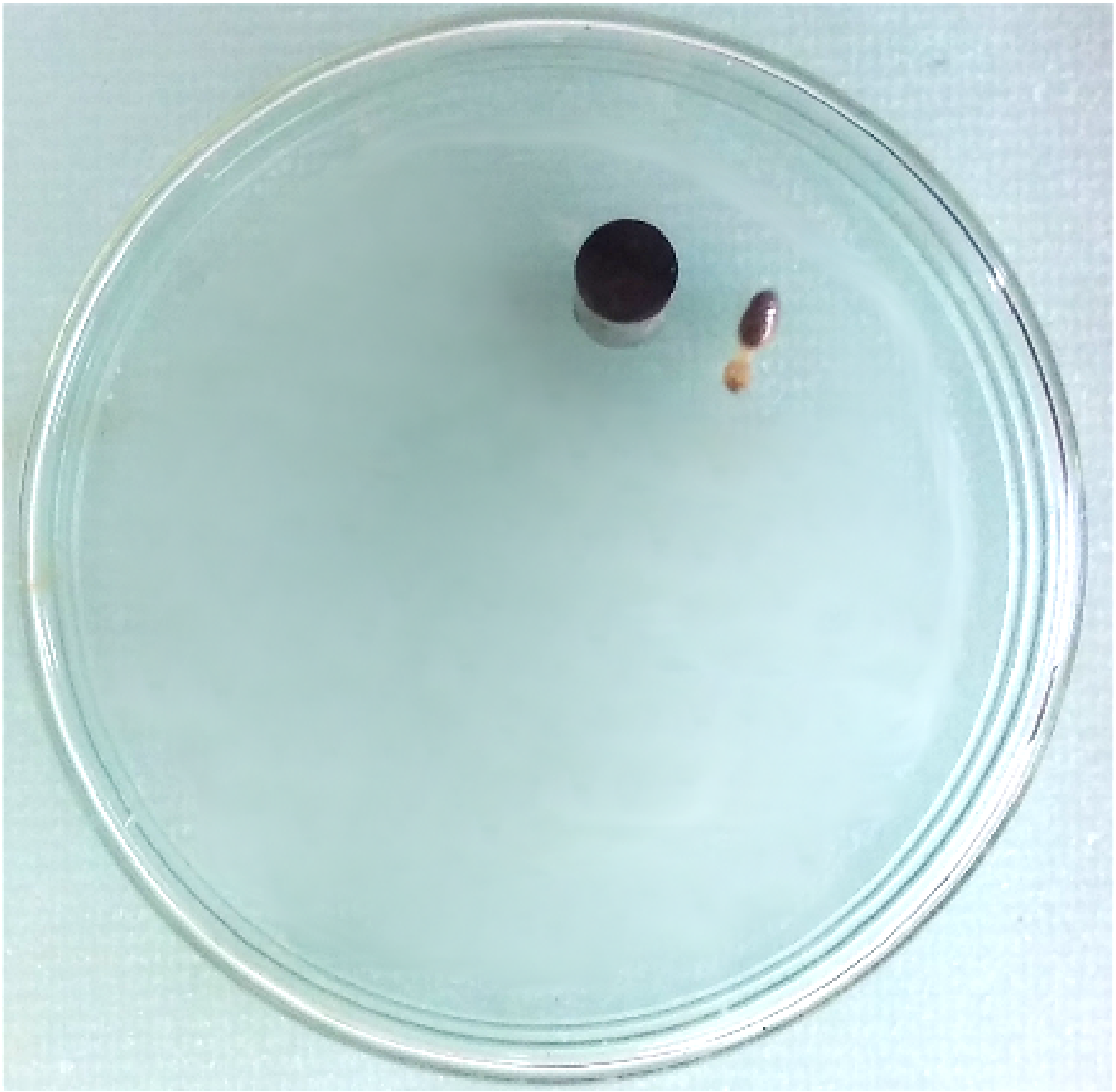

Fig. S3. One individual can be seen while exploring an arena with metal poles on it as obstacles in order to simulate the mechanical presence of other individuals. Arena diameter is 53 mm and the pole diameter is the same average length of an adult termite.

inert as not having smell that could attract (or repel) the termites. The height of the obstacles was chosen so they have about the same height as the Petri dish. If they were smaller, the termite could be able to climb it. The identical obstacles were glued following three different spatial configurations and a range of densities, as explained below.

Clustering configuration experiment. As a way to represent the space that would be occupied by the inert obstacles, a few experiments were performed with confined termites. In these experiments, termites were free to walk in the arenas and pictures of the typical pattern of the configuration of them were taken (Fig. S4). Inspired by these pictures, the obstacles were glued in the positions indicated by the black dots in Fig. S5. This configuration is referred to as a "clustering pattern".

The arenas were prepared with the obstacles forming asymmetrical aggregates with different sizes, and small space between each obstacle. In some arenas, one or two obstacles were put apart from the cluster, again to make the configuration of the obstacles as similar as possible to real termite clustering configurations. In all cases of this configuration, the clusters did not

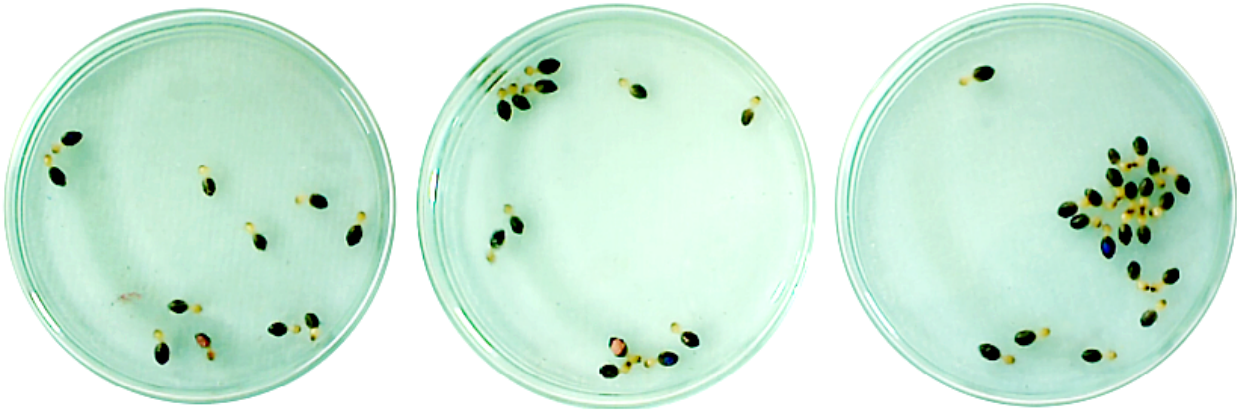

Fig. S4. Pictures of typical spatial distribution of confined termites forming groups, which motivated the clustering configuration of the obstacles experiment. At the left, there were no evident clusters and social interactions occurred in pairs mostly (11 individuals). At the center, 12 individuals formed small clusters, for example four individuals clustered at the top of the arena. At the right, 21 individuals in the container, exhibited few free walking individuals but also a large size social cluster.

touch the arena's walls, so the termite could also follow a large unobstructed path close to the arena border.

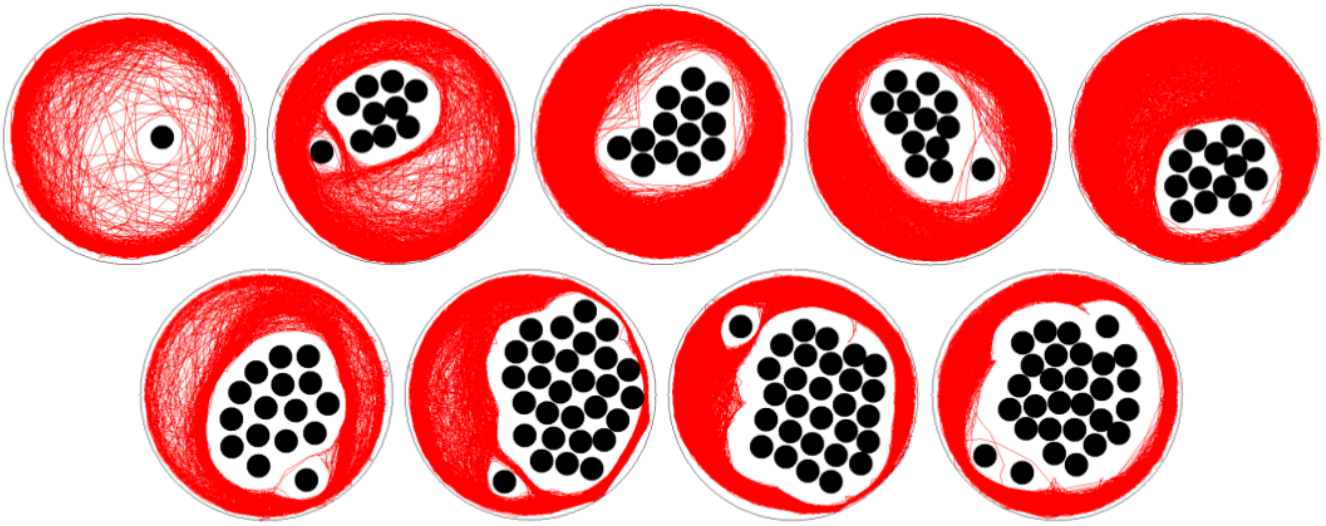

Fig. S5. Termite trajectories (red) for 1, 10, 13, 16 and 29 obstacles, placed following the clustering configuration. The black circles represent the real position and size of the obstacles. Notice that even that there was a fair amount of space between the obstacles, the individuals mostly avoided entering the clusters.

Examples of the arenas used in this clustering configuration experiment are depicted In Fig. S5, together with the trajectories of the termite (red) in each one of them. Black circles represent the real position (and size) of the obstacles. As the borders of the arena were unobstructed, individual workers walked close to the borders of the arena, apparently following this pattern most of the time. The free paths between the obstacles were rarely explored and, as expected, the termite largely ignored the obstacles spending little or no time trying to interact with them.

Obstacles distributed homogeneously. Obstacles placed homogeneously were explored as an alternative spatial configuration. As before, the borders of the arena were kept free of obstacles. However, in this configuration there are some wide paths between the obstacles, so it is expected that this can influence the walking patterns of the termite. Examples of termite trajectories are depicted in Figure S6 where termite trajectories in each arena, with 1, 10, 13, 16 and 29 obstacles, are depicted. As before, termite walked most of the time close to the arena border. It was observed that, until 16 obstacles, termites walk often between the obstacles, but beyond this number and particularly with 29 obstacles, inner incursions are scarce and termites walked almost entirely at the border of the arena.

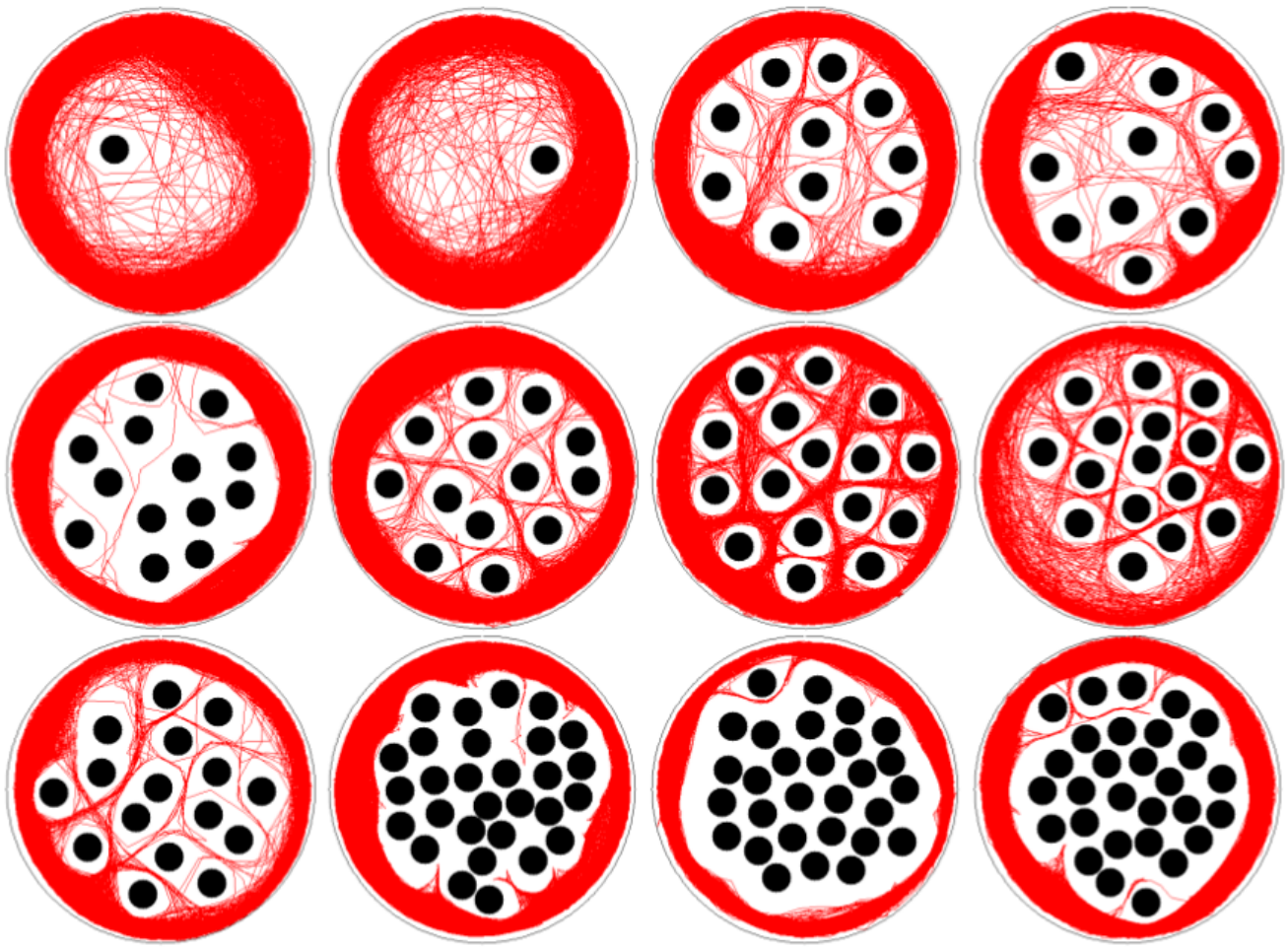

Fig. S6. Termite trajectories (red) are depicted for 1, 10, 13, 16 and 29 obstacles, placed in a random configuration. The black circles represent the real position and size of the obstacles.

Obstacles forming barriers at the border. Observations indicate that single termites walk mostly following the borders of the arena. As a way to modify this persistent behaviour, in our third spatial configuration experiment, the obstacles were placed forming barriers in radial directions. Here, the obstacles were glued close to the borders of the arena, as can be see in Figure S7 where the termite trajectory is represented in red and the black dots are the obstacles, as before. For this configuration, an atypical behaviour was observed. Most of the experiments failed, since the termite was very persistent trying to push or climb the obstacles. Eventually, the termites fell upside down and were unable to walk anymore. We succeed in registering only three cases were the termite actually walked along the container. The two first cases, where just one obstacle was put in the arena, had distinct outcomes. In the first case, the termite follows his trial most of the time, and it explored only a fraction of the available space. In the second case, almost all the arena was explored. One should mention that there was no significant difference between both experimental conditions (room temperature, luminosity, etc). In the last case, the termite did not engaged in trying to push away the obstacles and an intricate pattern resulted.

As a conclusion, if space restriction were to induce Lévy-like movements due to trajectory truncation one should identify Lévy walks as the density of obstacles increased. However, Levy walks were not evident in these experiments, independently of the configuration of the obstacles, as explained in the main text.

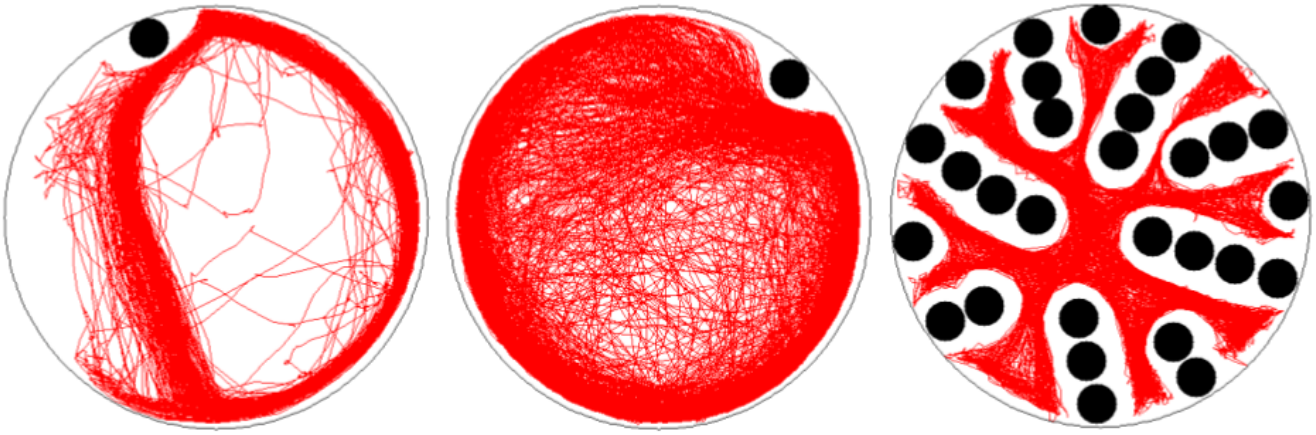

Fig. S7. Termite trajectories (red) for 1 and 29 obstacles, placed in the barrier configuration. The black circles represent the real position and size of the obstacles.

An agent based model for annular motion

Our agent-based model was inspired in the walking patterns of termite workers while freely exploring arenas formed by a bond paper of size A0. Figure S8 shows a typical trajectory registered with four thousand steps obtained from a termite walk after about 140 seconds of video recording. The arrow indicates the start point of the trajectory. It is easy to see that the termite follows a trajectory resembling a correlated random walk where a new step is in a direction very close to that of the preceding one and few cases with a large deviation (see three cases indicated by the red open circles in figure S8).

Figure S9 shows the typical distributions obtained for the step size and turn angles for a trajectory of a free termite walk. Notice that, the step length distribution is well fitted by a normal function. The mean step value is $\bar{\delta} = 1.1$mm and the standard deviation $\sigma = 0.4$mm. Notice as well, that for angles around zero we observed a good exponential fit although, for values of the turning angle above a value close to $\pi/2$ a deviation is observed. Above this value, an uniform value to the distribution is observed. In fact, the solid line in the figure S9 is a fit to the termite data using

$$F(\theta) = p_\theta + \frac{1}{\sigma_\theta\sqrt{2\pi}} \exp\left(-\frac{\theta^2}{2\sigma_\theta^2}\right) \qquad [1]$$

with $p_\theta = 0.01$ and $\sigma_\theta = 0.4$.

For simplicity, modeled termites are represented by circles of radius a. Termite can stay in two states: active or inactive. An active termite becomes inactive with a probability p_w and stays inactive by a time interval τ (waiting time) or with complementary probability $(1 - p_w)$ it tries to move. The waiting time is a random variable with a distribution that decays as a power-law with slope γ [1].

The walk of an active termite is described by a persistent random walk, in which the position of the ith termite at $(n+1)$th step is given by

$$\vec{r}_i{}^{\,n+1} = \vec{r}_i{}^{\,n} + \vec{dr}_i{}^{\,n+1}, \qquad [2]$$

where $\vec{dr}_i{}^{\,n+1}$, the $(n+1)$th step, is given by

$$\vec{dr}_i{}^{\,n+1} = \delta\cos(\theta_i^n + \eta_i^{n+1})\hat{i} + \delta\sin(\theta_i^n + \eta_i^{n+1})\hat{j} \qquad [3]$$

here δ is a random step size chosen from a Gaussian distribution, θ_i^n is the direction of the (n)th step and η_i^{n+1} is a random perturbation on the direction of the preceding step chosen $\in (-\pi, \pi)$ with probability p_θ according to a uniform distribution and with a complementary probability according to a Gaussian distribution. The figure S10 shows schematically a few steps of a walk. Notice that the trajectory becomes ballistic if the variance and $p_\theta \to 0$ or random if it $\to \infty$ and $p_\theta \to 1$.

The model evolution rules are as follows.

i) The waiting time of all inactive termite is updated (subtracted by $dt = 1/N$) and if it becomes less than zero the termite is activated.

ii) An active individual i is randomly selected. With probability p_w it becomes inactive and, with the complementary probability, it tries to perform a step according to the equation (2).

- Once in the AB model overlaps are forbidden, when the individual i met another j the walk is interrupted.
- And with a probability p_{crowd} both individuals become inactive with their waiting times τ_i and τ_j randomly obtained.

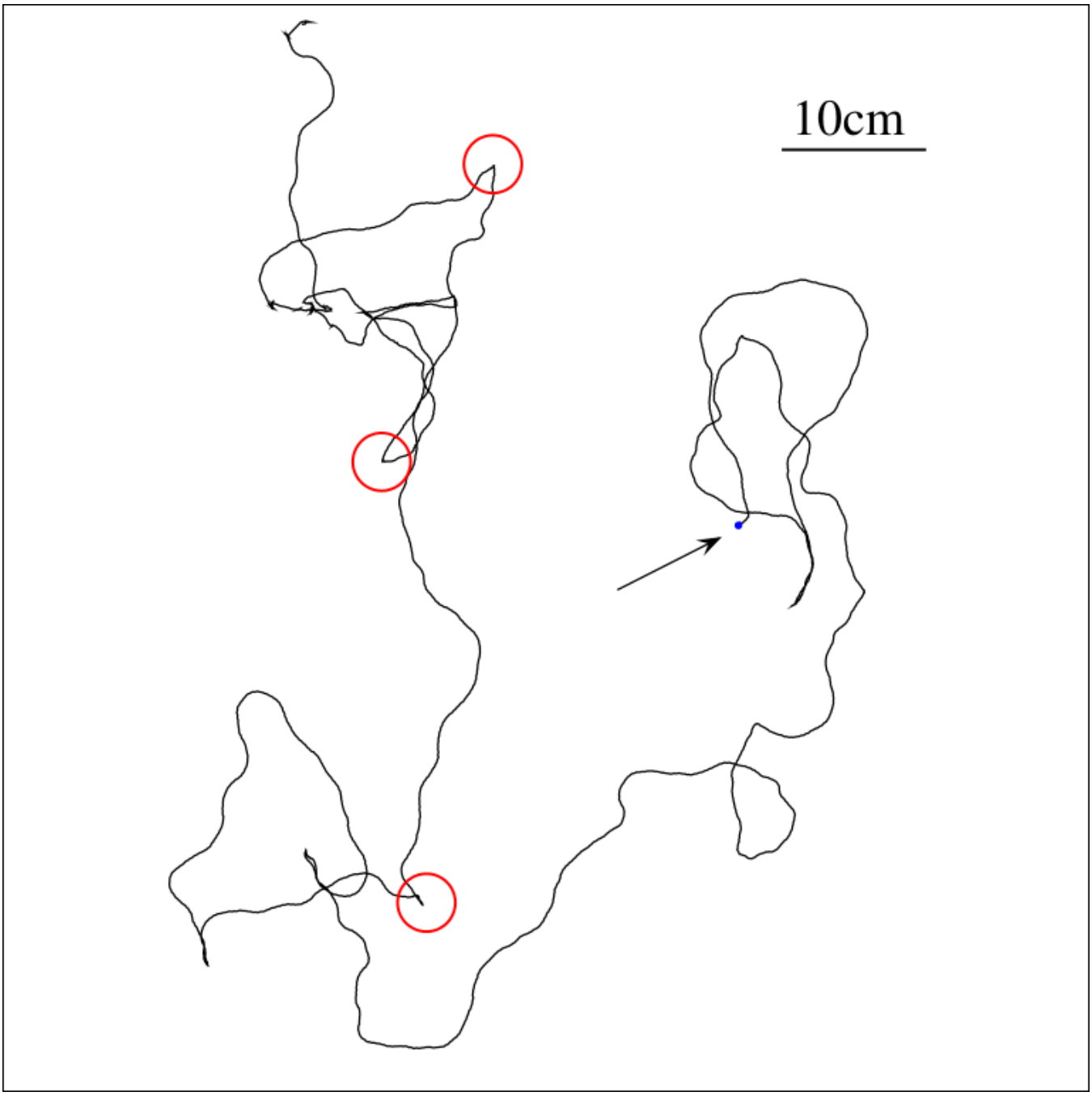

Fig. S8. A typical trajectory with four thousands frames on a free arena obtained after 140s. The arrow indicates the start point of the trajectory (blue circle). Three large deviations in the step direction are highlighted by open circles in red.

iii) The time is updated ($t = t + dt$), we return to the rule i and implement it iteratively.

The figure S10 shows a trajectory of one individual obtained on a free arena after four thousand steps. The trajectory is very similar to the termite in figure S8. The parameters used in the simulation were $\overline{\delta} = 1$, $\sigma = 0.4$, $p_w = 0$, $p_\theta = 10^{-2}$ and $\sigma_\theta = 0.4$.

Confined termites in an annulus configuration. The simulations are performed in a circular arena with diameter d and in an annulus (formed by two concentric circles) where N termites move (see VIDEO| 15:00 min, as an example). Initial condition are as follows. N termites are released at random positions on the arena (overlaps are forbidden) and its direction θ^0 is randomly chosen $\in [0, 2\pi)$. The state of each termite is set as inactive with probability p_w and the waiting time is chosen from the power-law distribution while another fraction is active. Trajectories obtained after 10^4 times step using 1, 2, 4 and 16 termites for circular and anular arenas are show in Figure S11.

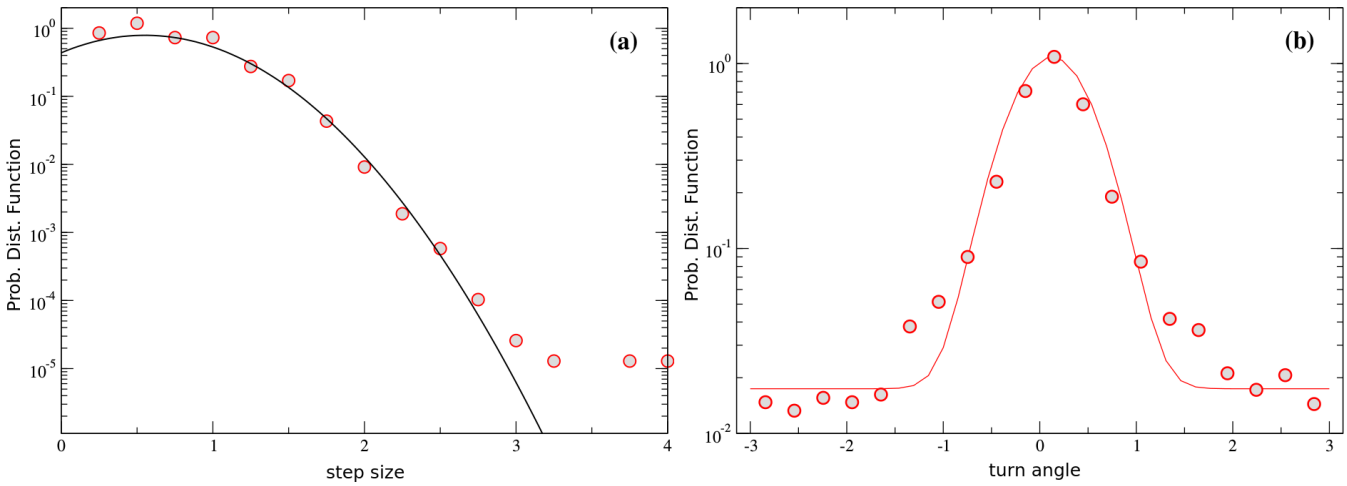

Fig. S9. Circles depict (a) the Probability distribution of step size and (b) the typical turning angle as measured from the trajectory of a termite worker moving freely in the arena. The fits are obtained using the equation 1 and the numerical data considering the proposed model for the termite walk.

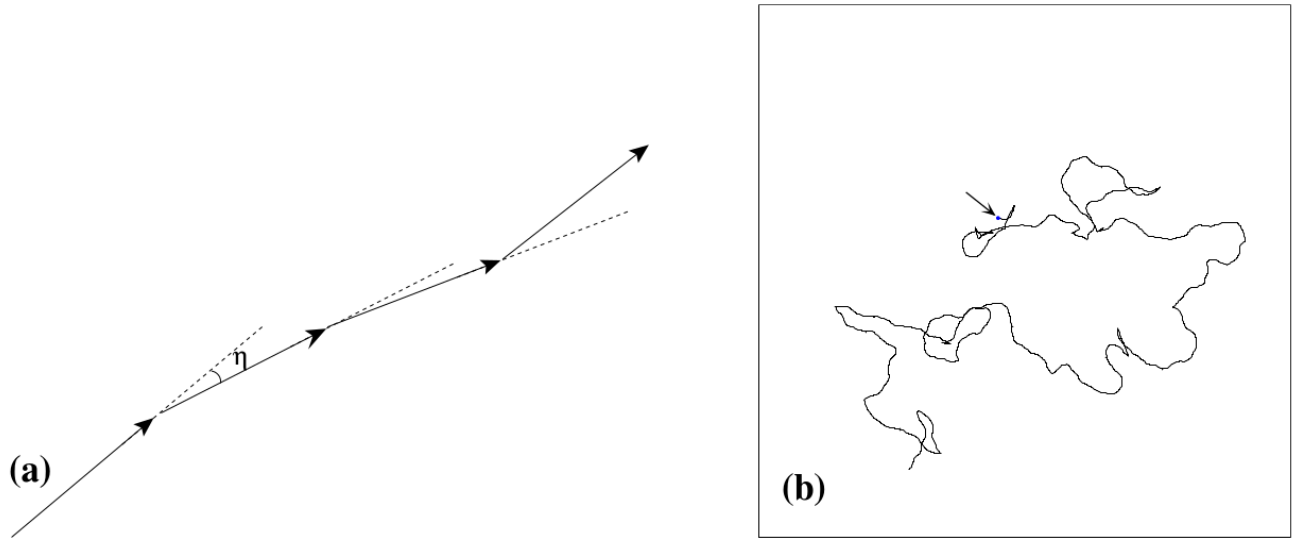

Fig. S10. (a) Schematic illustration of the trajectory rule. (b) A trajectory of a modeled termite on a free arena considering a walk with four thousand steps.

A solvable model for annular motion the emergence of Lévy walks in social groups with preferential attachments

Reynolds (2013)[2] showed how Lévy walks can emerge in social groups with preferential attachments. Here for completeness we briefly describe this model, as predicted dependency of the Lévy exponent, μ, on the number of preferential attachments matches our observations of termites. Model groups consist of an ignorant but responsive "leader" and its "followers". The leader is responsive to a small number, N, of its followers. The leader moves with constant speed and randomly selects a new direction of travel each time it encounters one of its followers –a collision avoidance response–; otherwise it continues to move with constant speed along a straight line. Immediately after each such turn the followers regroup around the leader. Follower movements comprise a superposition of a straight-line movement and a random walk which, unless stated otherwise, is a Brownian walk. The straight-line movement runs parallel to the leaders' movements and keeps pace with the leader. The orthogonal random movements result in occasional encounters with the leader. Analysis reveals that the distribution of distances travelled by the leaders (and so followers) between consecutive turns has a power tail with characteristic exponent $\mu = 1 + N/2$. These movement patterns correspond to a Lévy walk when $N <= 4$, and are consistent with our observations of confined termites.

Preferential interactions

Preferential interactions and individual recognition. As many other social insects, termites are able to recognize their nestmates which is important to maintain colony integrity in front of intruders and parasites. How this is achieved at the individual level?

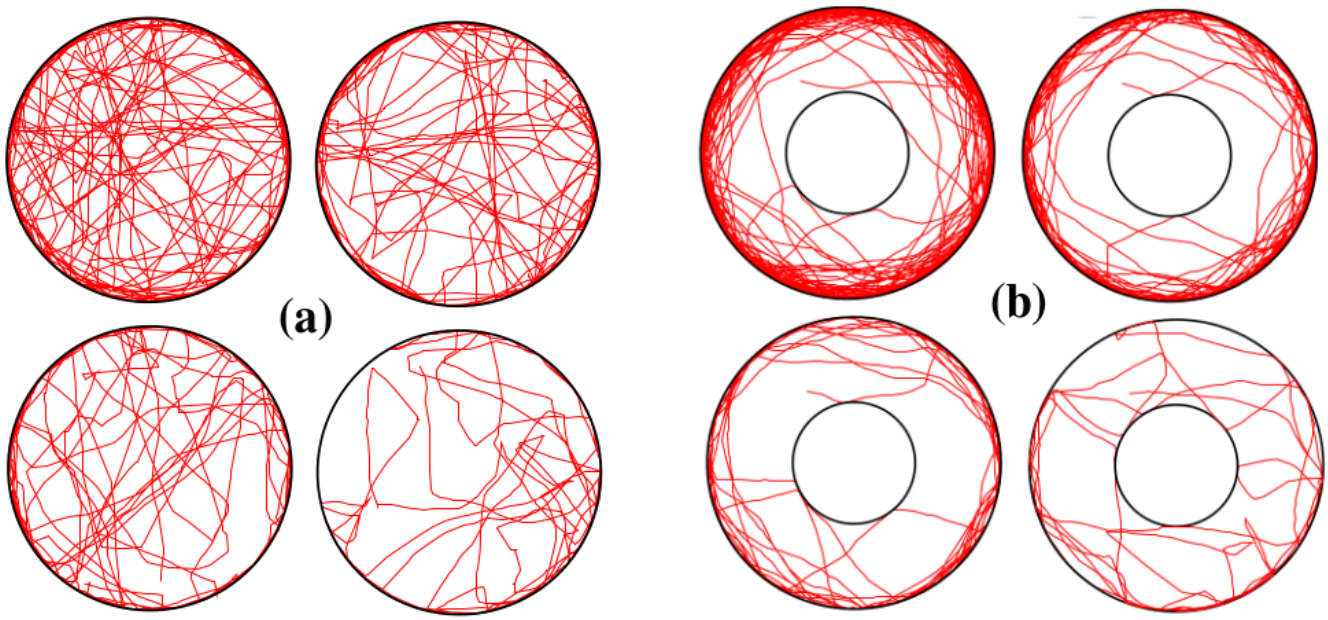

Fig. S11. (a) Trajectory of a termite after 10^4 times step on the circular (of diameter $10a$) and annulus (of inner $5a$ and outer $12a$) arena (b). The parameter used were $\sigma = 0.1$, $p_w = 0$, $p_{crowd} = 0$, $p_w = 0.01$, $p_\theta = 10^{-3}$, $\sigma = 0.2$ and $\overline{\ell} = 0.4$.

It is not very well understood. However individuals can easily recognize other individuals even from the same species but from different nests [4]. Another potentially interesting feature of insect social recognition would be ability to recognize specific individuals or specific groups. There is only one example of this reported in the literature and that is the case of the paper wasps [4] who apparently are able to identify facial features of specific individuals. This complex feature, it has been argued, may be associated with an increase of size and sophistication of brain structures, in a conjecture that is known as the *Social Brain Hypothesis* [5,6]. However there is limited evidence, at best, that termite brain has evolved large neuronal structures associated to individual recognition [7,8]. Moreover, it has been speculated that the ability of individual recognition and the memory involved in keeping a record of social acquaintances is also modulated by brain size in such a way that large brains give the opportunity of keeping in memory a large social network.

The average number of social acquaintances for a given individual –the Dunbar number [9]– is of about 150 in humans and would be less in species with less well endowed brains. With their tiny and barely unsophisticated brains, it would be almost impossible to think on a Dunbar number for them. However, we are reporting that social interactions among *C. cumulans* individuals seem to be selective and preferential, a feature not reported before with Dunbar-like numbers of less than 5 nestmates per individual as concluded from the above model and the experimental observations of preferential interactions with the methodology described below.

Experimental evidence of preferential interactions in termites. To retrieve termite positions from the experimental arenas we built a custom video tracking algorithm on top of open-sourced libraries of the Python scientific computing ecosystem. The computer code is freely available at GitHub (https://github.com/dmrib/trackingtermites) with tracking examples as well. In summary, it works as follows.

Termite detection. The first step consists in informing to the tracking algorithm the initial position of each termite individual. This is accomplished with a manual selection screen where the first frame of the video under study is displayed to the user, who employs the computer mouse to draw a box around every termite of interest. After the selection, each box is automatically recorded under a unique identity that persists until the end of the algorithm's execution.

Here, some implementation details are needed to ease understanding of the posterior data analysis stage:

1. when the users selects a termite area, the bounding box is constrained to 16×16 pixels. This is done in order to have a fixed distance parameter for reporting encounters between individuals (please refer to the explanation on how to detect encounters for better detail).

2. we have empirically found that the tracking algorithm works very much better if we try to track the termite abdomen are instead of its entire body. This seems to be due to the fact that the abdomen area is seen by the kernelized filter as a more stable region leading to better prediction of its position

Computing positions. After the initial position of each termite is known, this information is fed into the KCF algorithm. It is important to notice here that even though the tracking of all the individuals happens in parallel, each individual is evaluated

by a different instance of the algorithm. There is no sharing of data or parameters between each execution thread.

In very broad terms, we can understand each instance as one task of learning a classifier capable of distinguishing the appearance of the object being followed from the background of each video frame. This classifier can be evaluated in the neighbouring areas of the subsequent frame so that to find the new region containing the object. Each detection provides a new image patch that can be used to update the model. Visually the process can be understood as in Figure S12.

Although effective in most of the duration of the footages, some errors can arise from the temporary occlusion of the object being tracked (*e.g.*, by other termites, shadows in the arena, etc). To treat these cases, we introduced tools to let the user to interfere directly, manually resolving conflicts and errors. These tools are:

Frame rate control: the user can manipulate the minimal time interval required to change the frames displayed to the user to it is easier to visually inspect the progress of the tracking process and detect errors.

Restart tracking instance: the user is able to restart the tracker instance, putting it back in a coherent state right before errors had arisen.

Rewind to previous states: the user is able to rewind the tracking algorithm to a previous state, stopping the process, making necessary corrections to the bounding box and resume tracking.

The combination of the above features made this algorithm robust enough to handle the tracking of up to 120 termites simultaneously.

Detecting encounters. Since the termites' bodies are represented by a bounding box, an encounter between them would cause an intersection between these boxes area. By examining a posteriori all positions of each bounding box and expanding boxes to include the termite head, we can identify intersections and report the respective termite identities (Figure S13).

Statistical analysis of preferential attachments. Here we inspected whether termites walking in annular arenas would preferentially contact some of their nestmates over others along a *ca.* 30 min period. The step-by-step analysis and the full dataset are avaliable at Harvard Dataverse: https://doi.org/10.7910/DVN/7USPOA.

To do so, we filmed and tracked each individual termite in the confined group, tallying the number of time-steps this focal termite spent contacting a given target termite along the whole footage. This has produced a dataset such as:

```
Tallied time-steps for a group of 3 individuals.
-------------------------------------------------
  trajectory focalTermite targetTermite steps
1  traj00006    termite01     termite02   640
2  traj00006    termite01     termite03   676
3  traj00006    termite02     termite01   635
4  traj00006    termite02     termite03   500
5  traj00006    termite03     termite01   702
6  traj00006    termite03     termite02   502
-------------------------------------------------
```

Then, for each individual we averaged number of time-steps it acted as a target of an interaction along the whole footage, producing a result such as:

```
Averaged time-steps a termite spent as a target.
------------------------------------------------
  targetTermite steps
1     termite01 668.5
2     termite02 571.0
3     termite03 588.0
------------------------------------------------
```

Then, we ran a Chi-square test to verify whether the proportion of time-steps spent as a target would vary among termite individuals. That is to say, we inspected whether these proportions would depart from an uniform distribution and, if so, to point to the existence of 'favourite targets'.

In case the Chi-square test did point to significant differences, we counted the number of 'favourites' within that given group. These 'favourites' were defined as being the termites whose average number of time-steps spent as a target was larger than the global average of targeting time-steps in the whole footage.

The number of preferred target-termites in each arena (y-var) was then regressed against the number of termites therein confined (x-var), in order to inspect how preferential attachments would correlate with group size. Analysis consisted in contrasting the model thereby obtained with a model with zero intercept and slope = 1, that is, a model in which favouritism was absent. Modelling was performed in R, under Generalised Linear Modelling and normal error distribution, followed by residual analysis. Contrasts were made using Akaike Information Criterion (AIC).

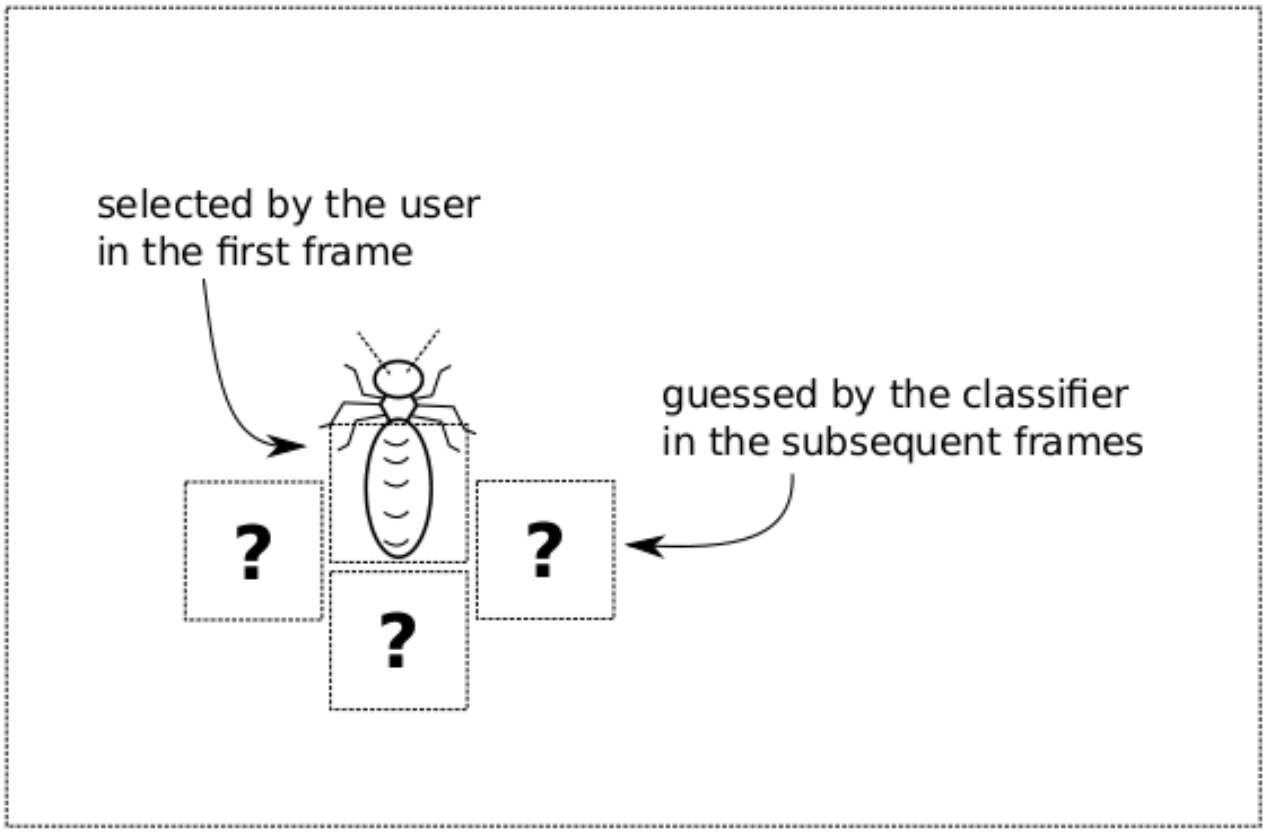

Fig. S12. The tracking process by means of bounding boxes: (i) the user manually draws a box encompassing the termite's abodomen; (ii) a classifier is trained to discriminate between areas containing the object and the background; (iii) the classifier evaluates the neighbourhood around the last known location of the object and the region with higher probability of containing the object is reported; (iv) a new classifier is trained with the new position; (v) the process is repeated until the end of the video. Termite drawing modified from DeSouza (2018)[10]. Arthropod drawings at Zenodo. http://doi.org/10.5281/zenodo.1318188

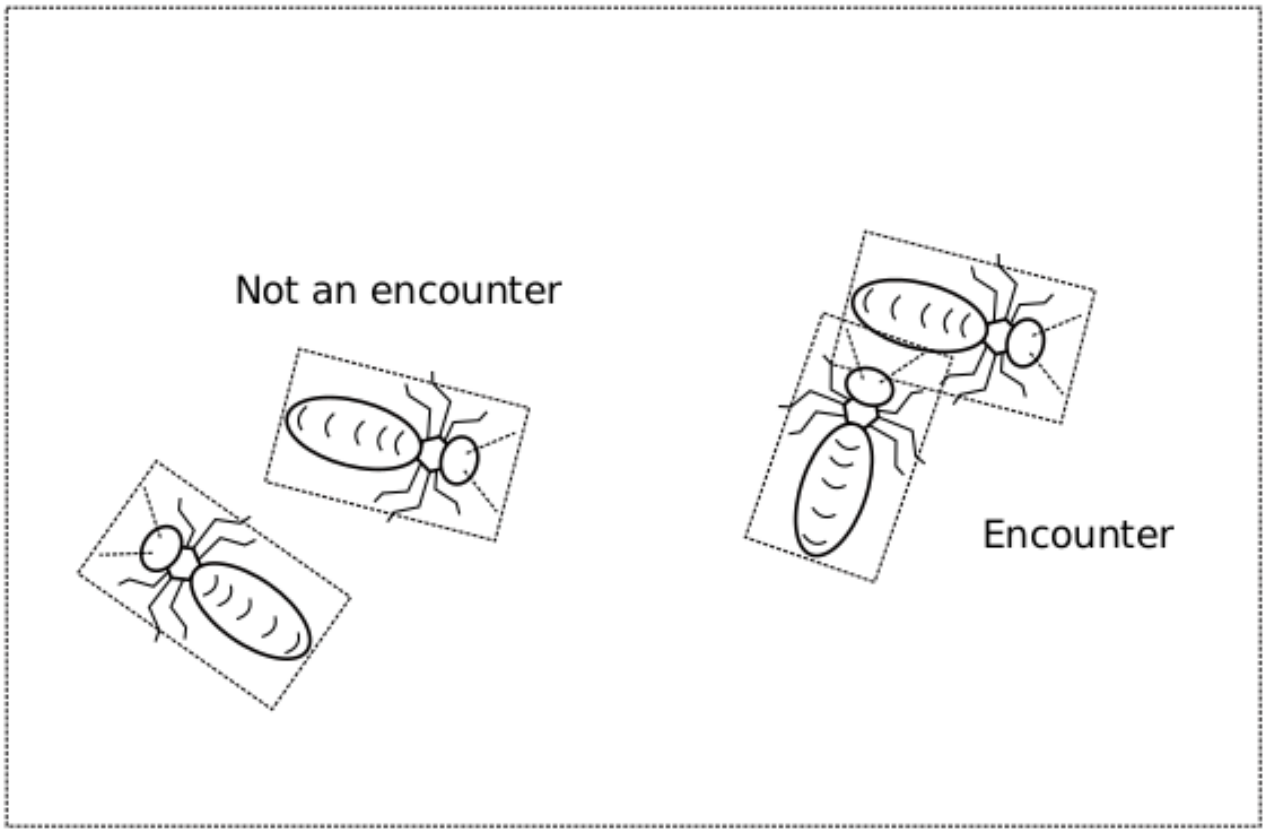

Fig. S13. Detecting encounters by recording bounding boxes intersections. Termite drawings modified from DeSouza (2018)[10]. Arthropod drawings at Zenodo. http://doi.org/10.5281/zenodo.1318188

More on power-laws in models and real termite data

Consider the fact that the turning points on a termite walk define a dimensionless time series, $u(t)$: u(t)=1 if a turn occurred at time t otherwise u(t)=0. The net displacement, n(t), of the time series u(t) is given by the running sum n(t)=$\sum_{t'=0}^{t} u(t')$. If the values of n(t) are completely uncorrelated and behave like "white noise", then the root-mean-square value of the running sum $F = \sqrt{\langle(\Delta n(t) - \langle\Delta n(t)\rangle)^2\rangle} \propto t^{\alpha}$ where α=1/2 and where $\Delta n(t) = n(t) - n(t + t_0)$. The angular brackets denote an average over all possible times t_0 [11]. Short-term correlations in the data may cause the initial slope of a plot of log(F)/log(t) to differ from 1/2, although it will still approach 1/2 at longer times. Consequently, Markov processes also give $\alpha = 1/2$ for sufficiently large t. Long-term power-law correlations [11] however, will generate α values $\neq 1/2$. Most of our data shows that $\alpha \approx 0.75$, and this implies that long term power-law correlations exist in the data, or in other words, the termite walking patterns were similar on all temporal scales.

On the other hand, mechanistic models that are essentially CCRW can converge on a Lévy motion distribution. Two cases are well documented. When searching for patchily distributed resources some foragers switch between extensive and intensive search patterns. This can result in bi-phasic walks with bi-exponential step-lengths that can resemble Lévy walks with power-law step-lengths [12](Benhamou, 2007). But close resemblance to a Lévy walks requires fine-tuning of the bi-exponential walk, i.e. fine-tuning of the distribution of search targets. The search targets in our study (conspecifics) are, however, uniformly distributed. Intrinsic multiphasic walks, so-called Weierstrassian random walks, that resemble Lévy walks have been identified in mud snails (*Hydrobia ulvae*) and in mussels (*Mytilus edulis*) [13-15]. These movement pattern appear to have their mechanistic origins in the coupling between neurobiology and motor properties and may be specific to organisms with stick-slip locomotion [15].

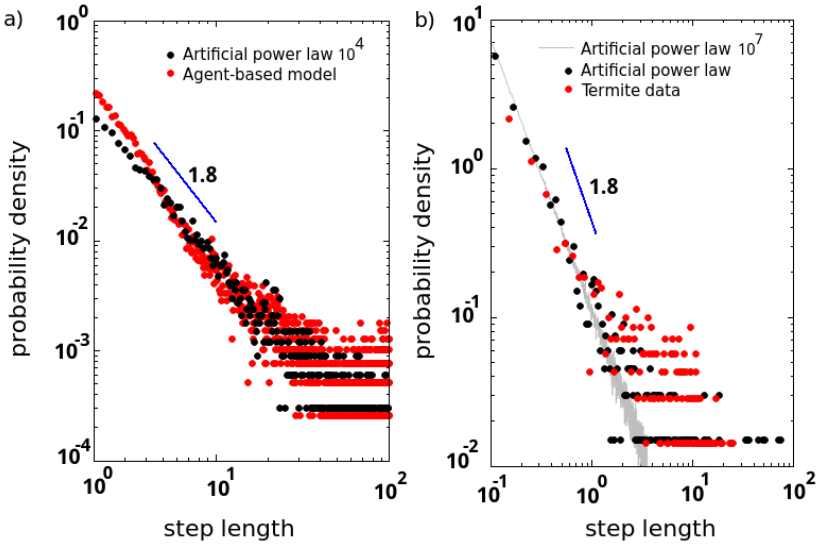

Fig. S14. artificial power law superimposed on (a) an agent-based and (b) on real termite data. See the text for more details.

We have plotted termite walking step distributions as accumulated plots because this is the preferred way of doing it in order to avoid the binning issues of a frequency plot (Figures 1 and 5, in the main text). We advise against presenting frequency plots when the time series are not long enough. We have presented frequency plots in Figure 3 of the main text since these are model data and so can be of an arbitrary length (10^7 points), binning in this case is not a significant problem, especially if they are presented more in a qualitative way. it may be interesting, nevertheless, to directly compare frequency plots for a qualitative visual comparison. Consider Figure S14(a) where we have matched fairly precisely an example of a segment from a step length distribution coming from the agent-based model (red, 10^5 points) and an artificially generated smooth power-law with scaling exponent -1.8 (black, 10^5 points). In Figure S14(b) we show the same smooth artificial power law with scaling exponent -1.8 of length 10^7 (grey) superimposed on the frequency distribution of the termite data (red, 1500 points) and a short artificially generated power law (black, 1500 points) in order to show how well they match the fluctuations of a pure power law behavior. As said before, the correct way of presenting step-length distributions is by means of the accumulated plot when a careful measure of the scaling exponent is needed.

Movies

Movie S1. Termite social clustering, available at https://lape.fisica.unam.mx:/termite/social_clustering.mp4

Movie S2. Termite social trapping in large container, available at https://lape.fisica.unam.mx:/termite/large_container.mp4

SI References

[1] Miramontes, O., DeSouza, O., Paiva, L. R., Marins, A. & Orozco, S. Lévy flights and self-similar exploratory behaviour of termite workers: beyond model fitting. PloS one 9 , e111183 (2014).

[2] AM Reynolds. Effective leadership in animal groups when no individual has pertinent information about resource locations: How interactions between leaders and followers can result in Lévy. EPL (Europhysics Letters) 102 (1), 18001 (2013).

[3] Marins A, DeSouza O. Nestmate recognition in *Cornitermes cumulans* termites (Insecta: Isoptera). Sociobiology. 2008 Jan 1;51(1):255.

[4] Tibbetts EA. Visual signals of individual identity in the wasp *Polistes fuscatus*. Proceedings of the Royal Society of London. Series B: Biological Sciences. 2002 Jul 22;269(1499):1423-8.

[5] Dunbar RI. The social brain hypothesis. Evolutionary Anthropology: Issues, News, and Reviews 1998;6(5):178-90.

[6] Lihoreau M, Latty T, Chittka L. An exploration of the social brain hypothesis in insects. Frontiers in physiology. 2012 Nov 27;3:442.

[7] Gronenberg W, Riveros AJ. Social brains and behavior: past and present. Organization of insect societies: from genome to sociocomplexity. 2009:377-401.

[8] Farris SM. Insect societies and the social brain. Current opinion in insect science. 2016 Jun 1;15:1-8.

[9] Dunbar R. How many friends does one person need?: Dunbar's number and other evolutionary quirks. Faber & Faber; 2010 Mar 4.

[10] DeSouza O. Arthropod drawings. Zenodo. Jul 2018. DOI 10.5281/zenodo.1318188. URL https://doi.org/10.5281/zenodo.1318188

[11] Peng, C. K., J. M. Hausdorff, J. E. Mietus, S. Havlin, H. E. Stanley, and A. L. Goldberger. 1995. "Fractals in physiological control: from heartbeat to gait". Pages 313-330 in G. M. Zaslavskii, M. E. Shlesinger and U. Frisch, editors. *Levy Flights and Related Topics in Physics*. (Springer-Verlag, Berlin).

[12] Benhamou, S. How many animals really do the Lévy walk? Ecology 88,1962–1969 (2007).

[13] Kölzsch, A. et al.. Experimental evidence for inherent Lévy search behaviour in foraging animals., Proc., Roy. Soc. B 282, 20150407 (2015).

[14] Reynolds, A.M. Mussels realize Weierstrassian Lévy walks as composite correlated random walks., Sci. Rep. 4, article 4409, (2014).

[15] Reynolds A.M., Bartumeus F, Kölzsch A, van de Koppel J. Signatures of chaos in animal search patterns. Scientific Reports 6, 23492 (2016)